

Non-perturbative Renormalization of Improved Staggered Bilinears

Andrew T. Lytle*

School of Physics and Astronomy, University of Southampton, Southampton SO17 1BJ, UK

E-mail: atlytle@gmail.com

Stephen R. Sharpe

Department of Physics, University of Washington, Seattle WA 98195-1560, USA

E-mail: srsharpe@uw.edu

We compute Z -factors for general staggered bilinears on fine ($a \approx 0.09$ fm) MILC ensembles using both asqtad and HYP-smearred valence actions, comparing the results to the predictions of one-loop perturbation theory. This is an extension of previous work on the coarse ($a \approx 0.12$ fm) MILC ensembles. It provides a laboratory for studying NPR methodology in the staggered context, and is an important stepping stone for fully non-perturbative matching factors in ongoing computations of B_K and other weak matrix elements. We also implement non-exceptional RI/SMOM renormalization conditions using the asqtad action and present first results.

The 30th International Symposium on Lattice Field Theory

June 24 – 29, 2012

Cairns, Australia

*Speaker.

1. Introduction

Renormalization of lattice operators is an essential component for many precision applications of lattice QCD. Amongst these are the determination of quark masses and weak interaction phenomenology, both of which require matching operators to continuum renormalization schemes.

Non-perturbative renormalization (NPR) [1] is a technique for performing such matching calculations using lattice simulations directly, and does not require the use of lattice perturbation theory. Instead, it requires that the renormalization scale μ is well separated from both the cutoff scale of the simulation, $1/a$, and the scale at which non-perturbative QCD effects become significant:

$$\Lambda_{\text{QCD}} \ll \mu \ll 1/a. \quad (1.1)$$

There are relatively few NPR studies using staggered fermions [2, 3, 4, 5, 6]. We have calculated matching factors for all staggered fermion bilinears spread over a 2^4 hypercube, determining their renormalization scale dependence and comparing them to the predictions of one-loop lattice perturbation theory (PT) [7]. We use both HYP-smeared and asqtad valence fermions on an asqtad sea. Previously we used the MILC coarse ensembles [5]; here, in Section 2, we extend the results to the fine lattices.

The bilinear operators form the building blocks for the four-quark operators used for weak interaction phenomenology. An ongoing computation of B_K using HYP-smeared staggered fermions finds $\hat{B}_K = 0.727 \pm 0.004(\text{stat}) \pm 0.038(\text{sys})$ [8]. The dominant error comes from using the one-loop perturbative matching factor, and is estimated to be 4.4% assuming that two-loop effects are of size α^2 . The present work is an important first step towards fully non-perturbative matching, which will both reduce the error and improve its reliability. The current study will give a general indication of how accurate one-loop predictions are, and thus indicate the reliability of the error estimate used in [8]. The bilinears are also of phenomenological interest in their own right for the determination of quark masses.

The asqtad light-quark matching factor Z_m was calculated non-perturbatively in [3], using the RI/MOM scheme. It is however advantageous to use a matching scheme that is less sensitive to the effects of low-energy QCD. In Section 3 we present results for the scalar and pseudoscalar bilinear channels using the RI/SMOM scheme. We find a significant reduction in non-perturbative splitting between these channels and weaker mass dependence relative to the RI/MOM case.

2. Exceptional NPR

We compute bilinear Z -factors for all spin (γ_S) and taste (ξ_F) structures. These fall into 35 irreducible representations (irreps) under the lattice symmetry group, which are enumerated in Table 1. Unlike with Wilson or domain wall fermions, staggered bilinears are slightly non-local, spread over a 2^4 hypercube and requiring gauge links in their definition. Their connection with the continuum bilinears may be expressed as follows:

$$\overline{Q}(x)(\gamma_S \otimes \xi_F)Q'(x) \cong Z_{\gamma_S \otimes \xi_F} \sum_{A,B} \overline{\chi}_A(n) \overline{(\gamma_S \otimes \xi_F)}_{AB} U_{n+A,n+B} \chi'_B(n). \quad (2.1)$$

Here $\chi_A(n)$ is a single-component field located at site $n+A$, where n labels the hypercube and A a site within the hypercube. The $Q(x)$ are four-component Dirac spinors that also come in

# links	S	V	T
4	$(\mathbf{1} \otimes \xi_5)$	$(\gamma_\mu \otimes \xi_\mu \xi_5)$	$(\gamma_\mu \gamma_\nu \otimes \xi_\mu \xi_\nu \xi_5)$
3	$(\mathbf{1} \otimes \xi_\mu \xi_5)$	$(\gamma_\mu \otimes \xi_5) \quad (\gamma_\mu \otimes \xi_\nu \xi_\rho)$	$[(\gamma_\mu \gamma_\nu \otimes \xi_\mu \xi_5) \quad (\gamma_\mu \gamma_\nu \otimes \xi_\rho)]$
2	$(\mathbf{1} \otimes \xi_\mu \xi_\nu)$	$(\gamma_\mu \otimes \xi_\nu) \quad (\gamma_\mu \otimes \xi_\nu \xi_5)$	$[(\gamma_\mu \gamma_\nu \otimes \mathbf{1}) \quad (\gamma_\mu \gamma_\nu \otimes \xi_5)] \quad (\gamma_\mu \gamma_\nu \otimes \xi_\nu \xi_\rho)$
1	$(\mathbf{1} \otimes \xi_\mu)$	$(\gamma_\mu \otimes \mathbf{1}) \quad (\gamma_\mu \otimes \xi_\mu \xi_\nu)$	$[(\gamma_\mu \gamma_\nu \otimes \xi_\nu) \quad (\gamma_\mu \gamma_\nu \otimes \xi_\rho \xi_5)]$
0	$(\mathbf{1} \otimes \mathbf{1})$	$(\gamma_\mu \otimes \xi_\mu)$	$(\gamma_\mu \gamma_\nu \otimes \xi_\mu \xi_\nu)$

Table 1: Covariant bilinears forming irreps of the lattice symmetry group. Indices μ , ν and ρ are summed from 1 – 4, except that all are different. Pseudoscalar and axial bilinears are not listed: they can be obtained from scalar and vector, respectively, by multiplication by $\gamma_5 \otimes \xi_5$. Bilinears related in this way have the same matching factors. This operation also implies the identity of the Z-factors for the tensor bilinears within square brackets. Bilinears marked in blue are used as the denominators of the ratios discussed in the text.

four “tastes” (indices left implicit). $U_{n+A, n+B}$ is an average over all minimal length gauge paths connecting $n + A$ to $n + B$.

We compute quark propagators on coarse ($a \approx 0.12$ fm) and fine ($a \approx 0.09$ fm) MILC gauge ensembles, using both asqtad and HYP-smearing valence actions at three masses for which $am_{\text{val}} = am_{\text{sea}}$. The use of momentum sources results in small statistical errors with relatively few (~ 10) configurations. One feature that distinguishes NPR using staggered fermions is that for each physical momentum p , 16 inversions must be performed corresponding to $p + \pi A$ and the resulting momentum-space propagator is a 16×16 matrix.

The gauge links used in the the construction of the bilinears are smeared. For the HYP valence action we use HYP smearing; for the asqtad valence action we use “Fat 7 + Lepage” smearing.

We impose RI'/MOM renormalization conditions on the bilinears of Equation (2.1) for a number of physical momenta (~ 10) at each mass, and extrapolate these results to the chiral limit. The pseudoscalar channel has a non-perturbative $1/m$ dependence and we do not present the results for it here.

We present our comparisons to PT in terms of ratios of Z-factors with the same spin-structure but different tastes. This makes the perturbative predictions especially simple because the continuum running cancels in the ratio:

$$\frac{Z_{S \otimes F1}(p)}{Z_{S \otimes F2}(p)} = 1 + \frac{\alpha(\mu_0)}{4\pi} [C_{S \otimes F2}^{\text{LAT}} - C_{S \otimes F1}^{\text{LAT}}], \quad (2.2)$$

where μ_0 is on the order of the lattice scale and is not related to the renormalization scale p . Since the ratios calculated non-perturbatively are sensitive to lattice artifacts and low-energy effects of QCD, their variation with respect to p provides an indicator as to whether one is in the NPR window.

Results for the fine HYP and asqtad ratios at a single scale $p = 2.1$ GeV ($(ap)^2 = 0.81$) are presented in Figure 1 and Figure 2. The perturbative results are evaluated with $\alpha(3 \text{ GeV}) = 0.24$. For the HYP ratios, we see good agreement with PT for the vector, axial vector, and tensor ratios at around the percent level. The scalar channel shows agreement at the 5 – 10 % level. Similar results

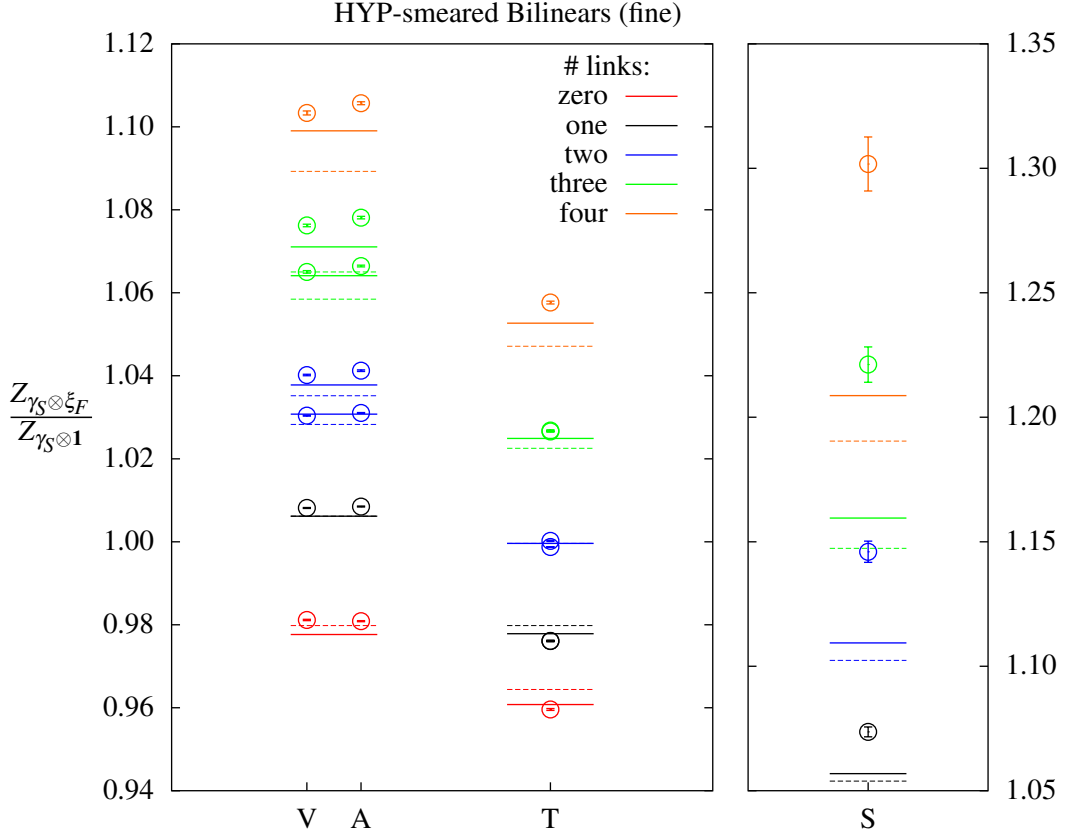


Figure 1: Comparison of Z-factor ratios for vector, axial, tensor and scalar bilinears to perturbation theory for HYP fermions on fine MILC lattices. Horizontal lines show perturbative predictions, with solid/dotted lines showing results with/without mean-field improvement. Results are in the chiral limit for the momentum described in the text.

were found on the coarse MILC lattices [5]. Overall, they indicate agreement at or better than the naive expectation of $\mathcal{O}(\alpha^2)$ truncation errors. The variation of these quantities with renormalization scale is shown in the left-hand column of Figure 3.

For the asqtad ratios, the vector, axial vector, and tensor agree with perturbation theory at the few-percent level, while the scalar ratios show significant discrepancy ($\sim 25\%$). The variation of these quantities with renormalization scale is shown in the right-hand column of Figure 3. For both the HYP and asqtad cases, the nonperturbative values in the scalar channel more nearly approach the perturbative predictions as $(ap)^2$ increases.

3. Non-exceptional NPR

Here we present our first results for staggered NPR using a non-exceptional scheme (RI/S-MOM) [9]. Non-exceptional schemes have reduced sensitivity to nonperturbative effects compared to their exceptional counterparts, increasing the range of the NPR window. They achieve this

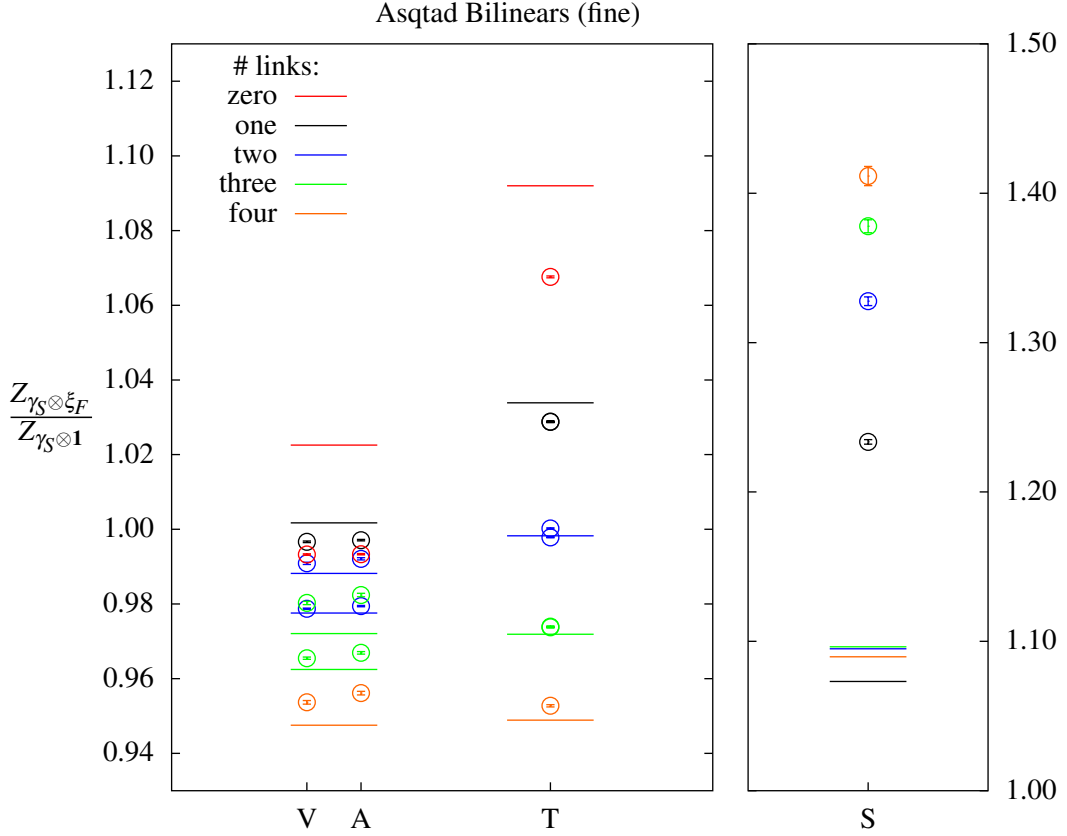


Figure 2: As for Fig. 1 except for asqtad fermions. Only results from mean-field improved PT are shown.

by using a kinematic setup that retains a single kinematic invariant but for which no channel has zero momentum flow (i.e. there are no “exceptional” channels). In the case of bilinears, the flow through the external quark lines satisfies $p_1^2 = p_2^2 = (p_1 - p_2)^2$. Figure 4a shows the nonperturbative splitting between the scalar and pseudoscalar channels in the exceptional and non-exceptional cases. Figure 4b compares the mass dependence of the scalar channel for the exceptional and non-exceptional cases. The non-exceptional setup has a much weaker mass dependence. This will improve the determination of Z_m using the asqtad action, where the strange sea-quark mass is fixed and cannot be extrapolated to zero.

4. Conclusion

We have presented non-perturbative matching factors for staggered bilinears using both HYP-smearred and asqtad valence actions, comparing our results to the predictions of one-loop perturbation theory over a range of momenta. We generally find good agreement (up to $\mathcal{O}(\alpha^2)$) for the Z-ratios presented here, except in the asqtad scalar channel (particularly for small $(ap)^2$).

We also present the first study of non-exceptional schemes using staggered fermions. We verify that nonperturbative splitting between the scalar and pseudoscalar channels is greatly reduced

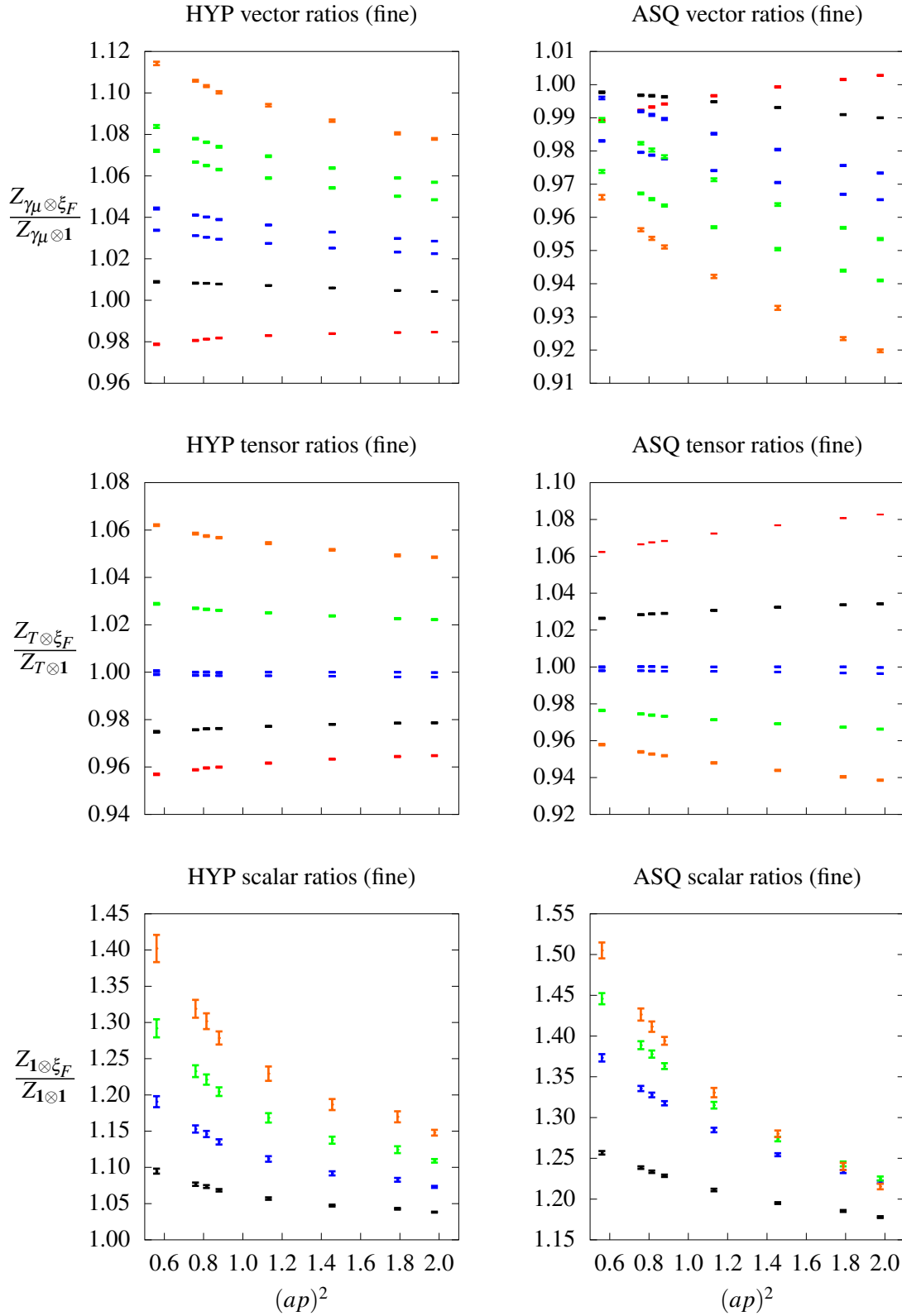
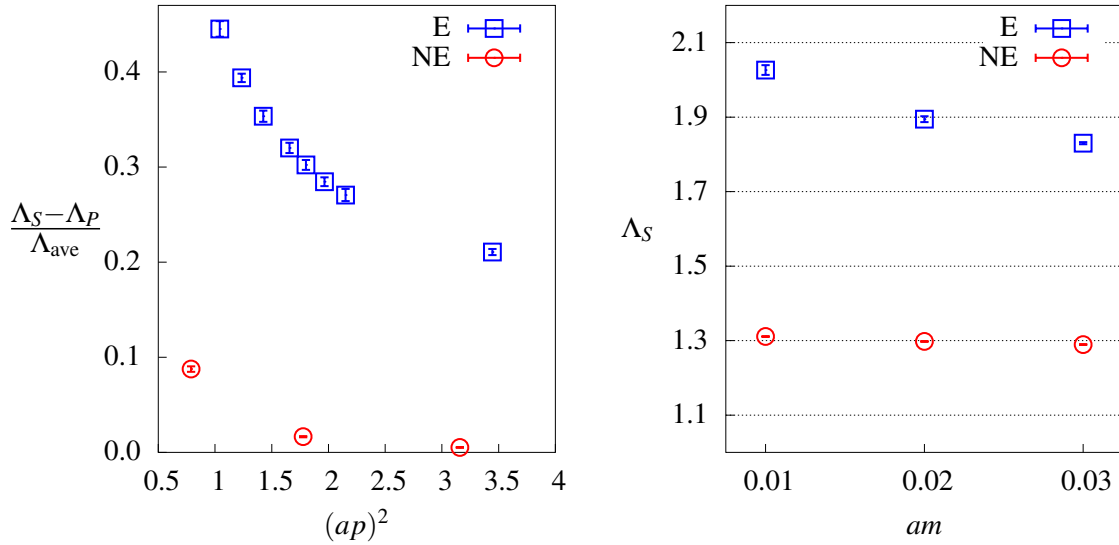


Figure 3: Momentum dependence of Z-ratios for HYP (left column) and asqtad (right column) fermions, calculated on fine MILC lattices. The colors correspond with those of the data plotted at a single scale in Figure 1 (HYP) and Figure 2 (asqtad).



(a) Non-perturbative splitting of the scalar and pseudo-scalar channels using an exceptional (E) and non-exceptional (NE) scheme. (b) Mass dependence of the scalar channel in the exceptional (E) and non-exceptional (NE) schemes.

relative to the exceptional case. The mass dependence of the scalar channel is also much milder, which should lead to an improvement in the determination of Z_m using this action.

Detailed descriptions of these results and associated theoretical work are in preparation [10].

5. Acknowledgements

The work of A. Lytle is supported by STFC grant ST/J000396/1. S. Sharpe is supported in part by the US DOE grant no. DE-FG02-96ER40956. Computations were carried out on USQCD Collaboration clusters at Fermilab. The USQCD Collaboration is funded by the Office of Science of the U.S. Department of Energy.

References

- [1] G. Martinelli *et al.*, Nucl. Phys. **B445**, 81-108 (1995). [hep-lat/9411010].
- [2] S. Aoki *et al.* [JLQCD Collaboration], Phys. Rev. Lett. **82**, 4392 (1999) [hep-lat/9901019].
- [3] A. T. Lytle, PoS **LAT2009**, 202 (2009), [arXiv:0910.3721 [hep-lat]].
- [4] A.T. Lytle, University of Washington Ph.D. thesis (2010), unpublished.
- [5] A. T. Lytle and S. R. Sharpe, PoS **LATTICE 2011**, 237 (2011) [arXiv:1110.5494 [hep-lat]].
- [6] J. Kim, B. Yoon and W. Lee, arXiv:1211.2077 [hep-lat].
- [7] J. Kim, W. Lee, S. R. Sharpe, Phys. Rev. **D83**, 094503 (2011). [arXiv:1102.1774 [hep-lat]].
- [8] T. Bae *et al.*, Phys. Rev. Lett. **109**, 041601 (2012) [arXiv:1111.5698 [hep-lat]].
- [9] C. Sturm *et al.*, Phys. Rev. D **80**, 014501 (2009) [arXiv:0901.2599 [hep-ph]].
- [10] A.T. Lytle and S.R. Sharpe, in preparation.